Chapter 3

Results and Discussion

Chemical Conversion of Labdane Diterpenes

3.1 The Corrected Stereochemistry of Labda-7,12(*E*),14-triene-17-oic Acid

Previously, we reported the structure of the labda-7,12(*E*),14-triene-17-oic acid (**14**) which was isolated from *C. oblongifolius* [8]. The structure was elucidated based on spectral data and by comparing them to those of the known labda-7,12(*Z*),14-triene [28]. In that report the absolute stereochemistry of diterpene **14** was proposed to be C5(*S*), C9(*R*), C10(*S*) (**14a**). However, from this study, the structure of compound **14** was reconfirmed by X-ray analysis and revised the structure to be *ent*-labda-7,12(*E*),14-triene-17-oic acid (**14b**) [29], thus, the absolute stereochemistry of **14** would assigned to have C5(*R*),C9(*S*),C10(*R*) configurations as depicted in Figure 3.1.

Labda-7,12(*E*),14-triene-17-oic acid (14a) *ent*-Labda-7,12(*E*),14-triene-17-oic acid (14b)

Figure 3.1

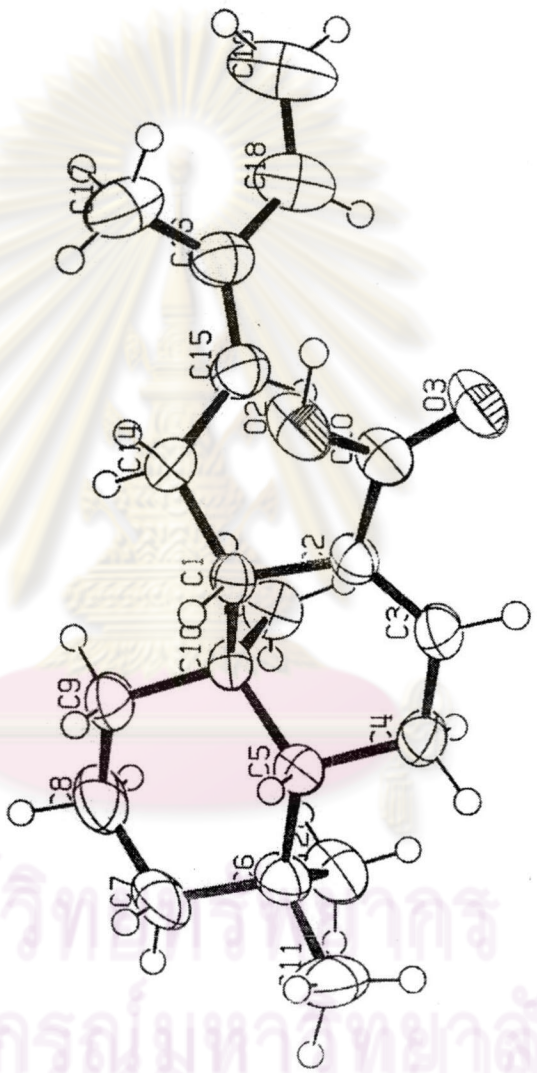

Figure 3.2 The structure of compound **14** from X-ray analysis.

3.2 Isolation and a preliminary biological activity test of labda-7,12(*E*),14-triene-17-oic acid (14)

As abovementioned, labda-7,12(*E*),14-triene-17-oic acid (**14**) along with three related derivatives were isolated from the stem bark of *C. oblongifolius* (collected from Prachaub Kirikhan province) as follows: the dried stem bark of *C. oblongifolius* (2.5 kg) was extracted with MeOH and the methanolic extract was concentrated under vacuum to obtain a dark-red gummy residue which was further partitioned with hexane to give a hexane extract. After removal of the solvent, the residue (40 g) was chromatographed over a silica-gel (SiO_2) column by stepwise gradient elution using hexane-EtOAc as solvent system to yield labdane diterpene **14** (23.64 g, 0.94%) along with hydrocarbon **11** (4.25 g, 0.17%), aldehyde **12** (1.60 g, 0.06%) and alcohol **13** (4.29. 0.17%) derivatives, respectively.

Although the structures of these four labdanes were established by spectroscopic methods and X-ray crystallographic determination, their biological activities have yet not been investigated. So, in order to investigate the biological activities of this labdane series, particularly cytotoxic activity, the cultured murine leukemia P-388 cell line was chosen for a preliminary test. Moreover, their activities on anti-platelet aggregation were also examined here.

As shown inTable 2.1, diterpene **12** and **13** were moderately active against P-388 cell line, while diterpene **11** was weakly active, and diterpene **14** was very slightly active. In the case of bioassay of anti-platelet aggregation, all of the compounds were found to be inactive or very slightly active except the diterpene **12**, which showed weak activity.

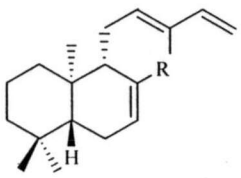

11, R = CH_3
12, R = CHO
13, R = CH_2OH
14, R = CO_2H

Table 3.1 Biological activities of diterpenes **11-14**.

Diterpene	IC_{50} (μg/ml)	
	P-388 cell line	anti-platelet aggregation
11	16.42	33.00
12	3.17	7.12
13	3.80	19.36
14	28.05	N.A.[a]

[a] Not active.

Since labdane diterpenoids **11-14** showed weak to moderate activities against P-388 cell line, we anticipated that these labdanes and their modified substances should exhibit cytotoxic activities against other human tumor cell lines. Therefore, the chemical transformation studies of this type of labdane diterpene were undertaken by using labda-7,12(*E*),14-triene-17-oic acid (**14**) as a starting material because it could be easily obtained in sufficient quantities from the stem bark of *C. oblonglifolius*. In addition, the relationships between the chemical structures of labdanes **11-14** and the modified labdanes and their cytotoxicities will be discussed.

3.3 Chemical Transformation of *ent*-Labda-7,12(*E*),14-triene-17-oic Acid (14)

In order to synthesize new derivatives of labda-7,12(*E*),14-triene-17-oic acid (**14**), 2 pathway were planned ; a) the chemical modification of carboxyl group at C(17) position to its related compounds and, b) the conversion of labdane **14** into a naturally occurring labdane, (+)-limonidilactone (**33**).

3.3.1 Modification of carboxyl group of labdane 14

In the case of our study, the chemical transformation of carboxyl group of labdane **14** was classified into three types as follows:

(1) conversion into its corresponding methyl ester and alcohol derivatives.

(2) conversion into its corresponding amide and ester by using coupling reaction.

(3) the closure of 6-membered lactone ring by the reaction with functionalized C(11)

Thus, the methylation of labdane **14** was first carried out. Diazomethane (CH_2N_2) was chosen as the reagent for introduction of the methyl ester function. Diazomethane was generated from diazald (p-$CH_3PhSO_2N(NO)CH_3$) by treatment with aqueous sodium hydroxide. The diazomethane gas was carried to the reaction vessel directly by means of a stream of dry nitrogen according to the protocol described by Lambardi [30], which allowed the methylation to be performed conveniently and safely without the need of complex apparatus and the handling of unstable diazomethane. The reaction with compound **14** in dichloromethane at room temperature gave the corresponding methyl ester **47** as an oil in nearly quantitative yield (Scheme 3.1). The ^{1}H NMR spectrum of compound **47** showed notably a singlet signal of -OCH_3 at δ 3.59 ppm.

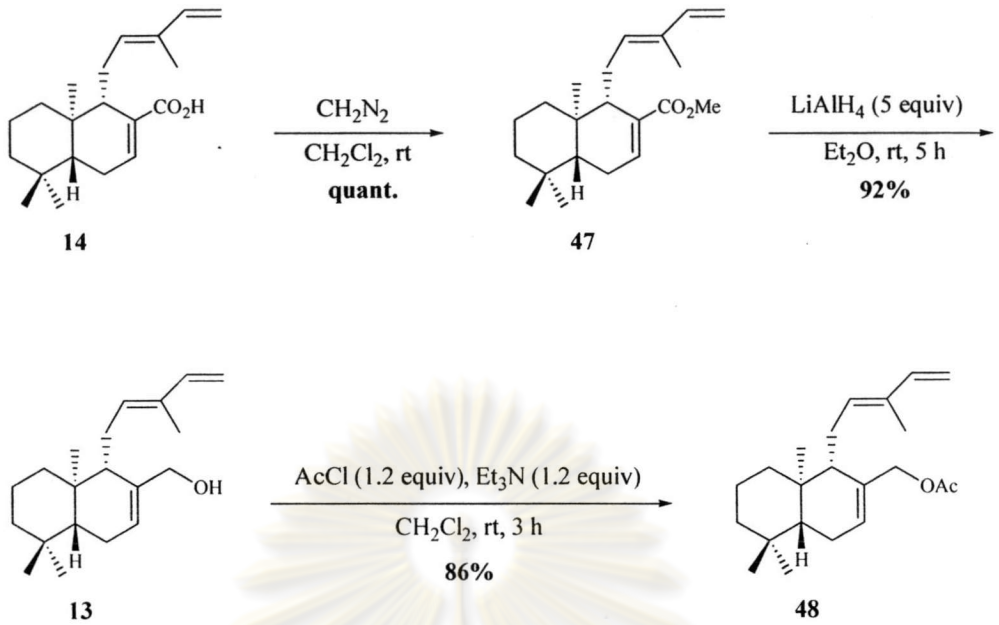

14 **47** **13** **48**

Scheme 3.1

To produce the acetate compound **48**, methyl ester **47** was reduced with an excess amount of $LiAlH_4$ in diethyl ether to provide alcohol **13** which was proved to be identical to that of a natural **13** by comparing the ^1H and ^{13}C NMR data. Subsequent acetylation of compound **13** by treatment with acetyl chloride in the presence of triethylamine as a base led to the desired product **48** in 86% yield as shown in Scheme 3.1. ^1H NMR ($CDCl_3$) showed notably a sharp singlet signal of an acetyl group at δ1.99 ppm and a marked down field of the H(17) resonance compared to the starting material **13** indicating that acetylation of the C(17)-OH group was occurred.

Based on the use of coupling reaction, the corresponding amide, N-[(*S*)-1-phenylethyl]-labda-7,12(*E*),14-triene-17-amide (**49**), was obtained in 79% yield upon exposure of carboxylic acid **14** to methylbenzylamine in the presence of DCC as a coupling agent and with a catalytic amount of DMAP (Scheme 3.2, eq. 1) [31]. Also, when compound **14** was allowed to react with 4-bromobenzyl alcohol under the same condition, the corresponding benzyl ester **50** was obtained in 86% yield (eq.2).

Their structures were confirmed by ^{1}H and ^{13}C NMR data.

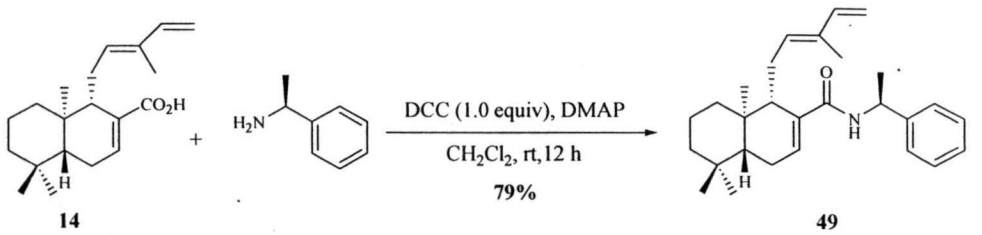

14 49 (eq. 1)

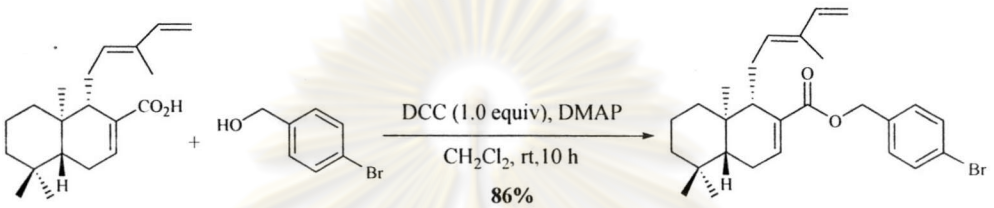

14 50 (eq. 2)

Scheme 3.2

Since it is known that the side chain of labdane-type diterpenes may be closed and opened with an oxygen atom as in manoyl oxide and its derivatives [32], the construction of 6-membered lactone ring by the reaction between the C(17) carboxyl group and the functionalized C(12) of labdane **14** was considered to perform to produce the new type derivatives. Then, it was found that lactone **51** and **52,** whcih structures containing allylic alcohol functional group were obtained in 63% and 28% yields, respectively, in one step upon treatment of **14** with *m*-CPBA in the presence of $NaHCO_3$ at 0 °C [33] as shown in Scheme 3.3. This is presumably due to successive oxirane-ring opening by carboxylate ion attack at C(12) position of the resulting epoxide after epoxidation. In addition, the lactone **53** was obtained in excellent yield (98%) by exposure of labdane **14** with TsOH in refluxing toluene for 7 h [23-24]. Their structures were confirmed by ^{1}H and ^{13}C NMR data, IR and mass spectroscopy.

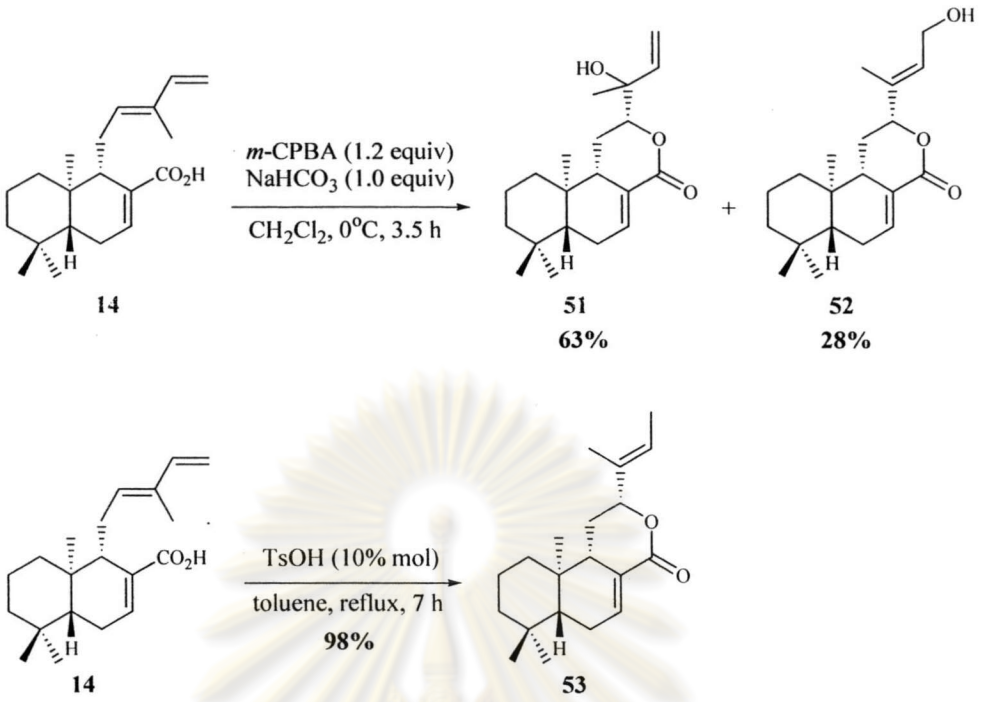

Scheme 3.3

The relative stereochemistry at C(12) position of these lactones was proposed based on the the NOE experimental data ($CDCl_3$) on lactone **52** and the results were consistent with the expected C12(*S*) configuration as shown in Table 3.2 and Figure 3.3.

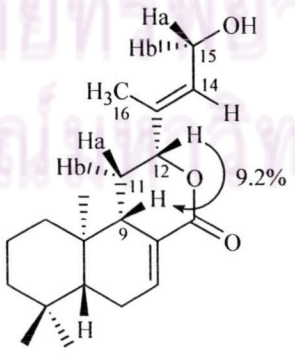

Figure 3.3 Diagram showing numbering systems on the lactone **52** and the NOE enhancement for selected pairs of protons.

Table 3.2 NOE experiments showing signal enhancement by irradiation at various protons of lactone **52**.

Irradiation at	Observed NOE (%)					
	H-9	H-11a	H-12	H-14	H-15a	H-16
H-12	9.2	3.7	0	11.7	-	1. 7
H-14	-	-	8.4	0	5.0	-
H-15	-	-	-	19.6	0	6.0
H-16	-	-	-	-	2.3	0

Irradiation at H(12) resulted in a significant positive NOE enhancement (9.2%) on the H(9) signal and *vice versa*. Thus this result confirmed the close proximity of these two protons, which can be possible only when the compound has a *syn* configuration. The NOE correlations between the pairs of protons H(12)-H(11a), H(12)-H(14), H(12)-H(16), H(14)-H(15), and H(15)-H(16) were also consistent with the proposed structure.

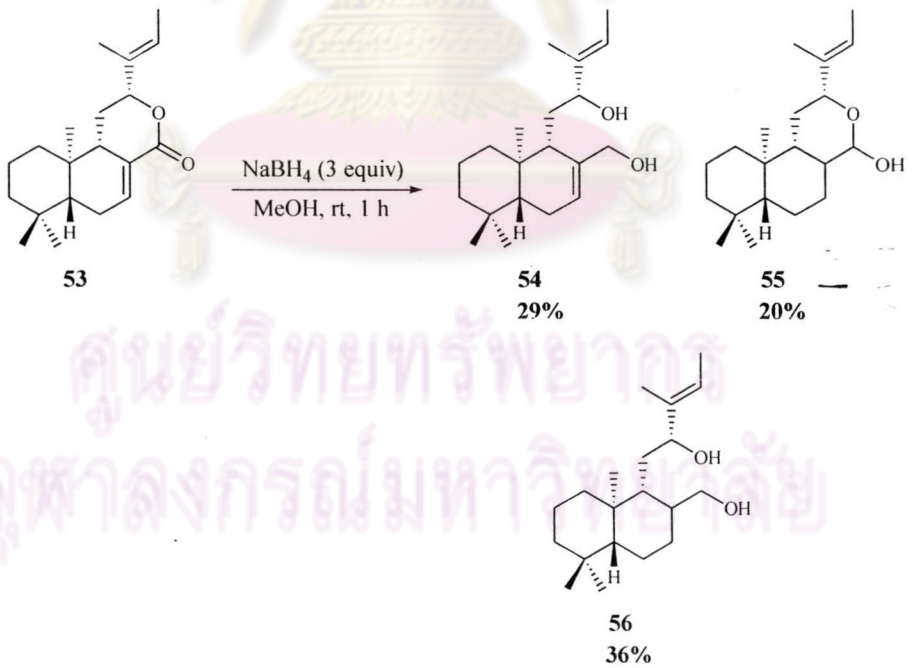

53

54
29%

55
20%

56
36%

Scheme 3.4

Having the lactone **53** in hands, we decided to synthesize another derivative by opening the lactone ring to a diol compound with some reducing agents. Unexpectedly, when lactone **53** was subjected to $NaBH_4$ reduction in MeOH at room temperature [34], it gave rise to the desired diol **54** only 29% yield in along with tricyclic products **55** and diol **56,** in 20% and 36% yields, respectively (see Scheme 3.4). The formation of **55** and **56** could reasonably be explained by the following mechanism (Scheme 3.5). The hydride ion (H^-) from $NaBH_4$ also behaved as a Michael donor and attacked at α,β-unsaturated ketone moiety to afford lactone **57.** Then, further reduction of **57** occurred to furnish diol **56** via aldehyde **59**, while compound **55** resulted from the proton abstraction of hemiacetal anion **58** from the solvent (MeOH) which occurred competitively with the opening of the lactone ring.

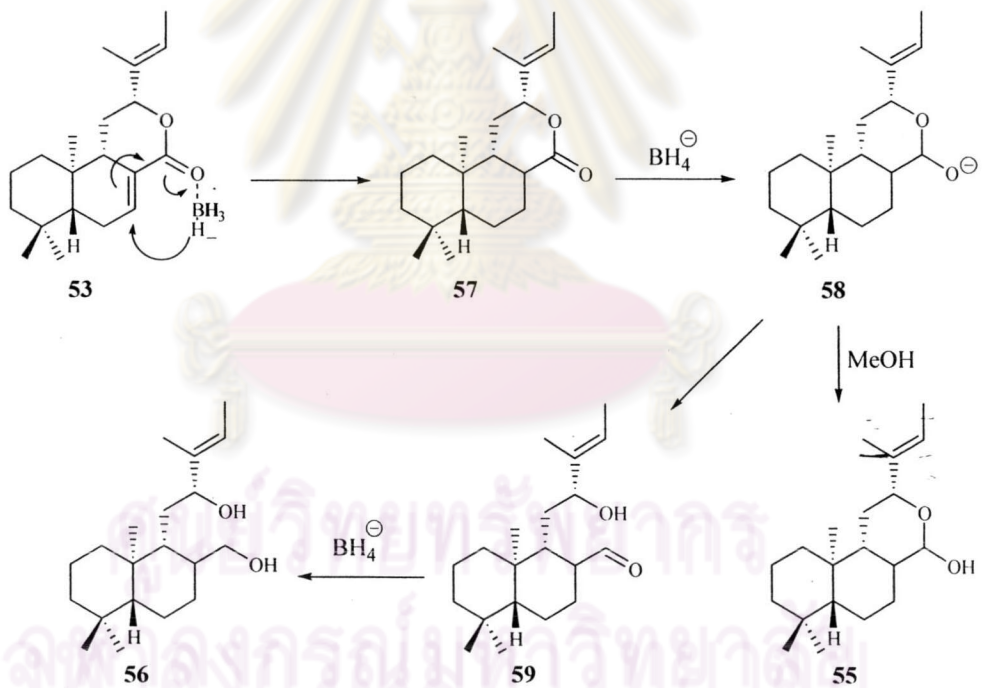

Scheme 3.5

3.3.2 Synthesie of limonidilactone (33)

We expected that limonidilactone (**33**) should exhibit anticancer activity owing to its unique structure bearing γ-butenolide and δ-lactone system. Thus, we decided to synthesize **33** by employing labda-7,12(*E*),14-triene-17-oic acid (**14**) as a starting material since stereochemistries at C(9) and C(10) of **14** were identical to those of the target product **33** as shown in Figure 3.4. To be accessible to limonidilactone (**33**), the retrosynthetic route as shown in Scheme 3.6 was undertaken.

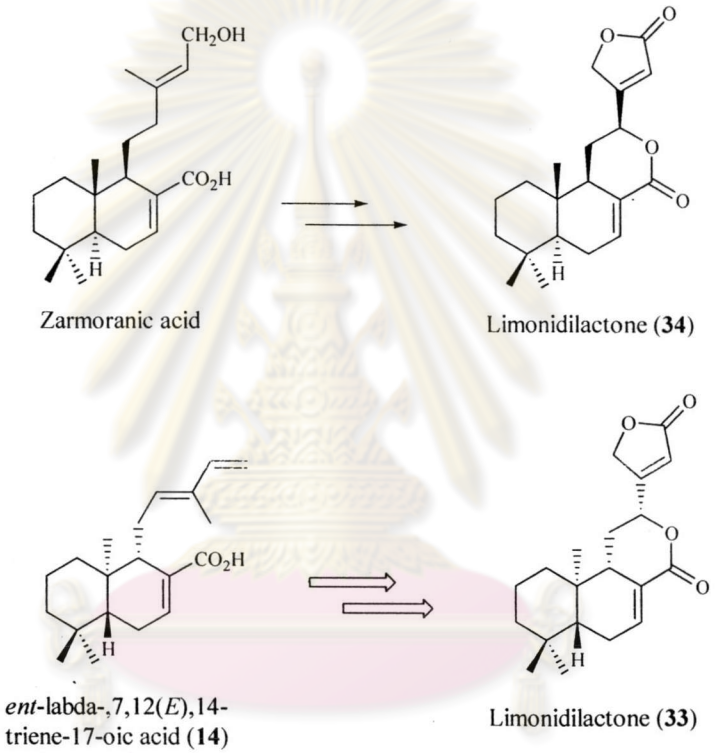

Figure 3.4

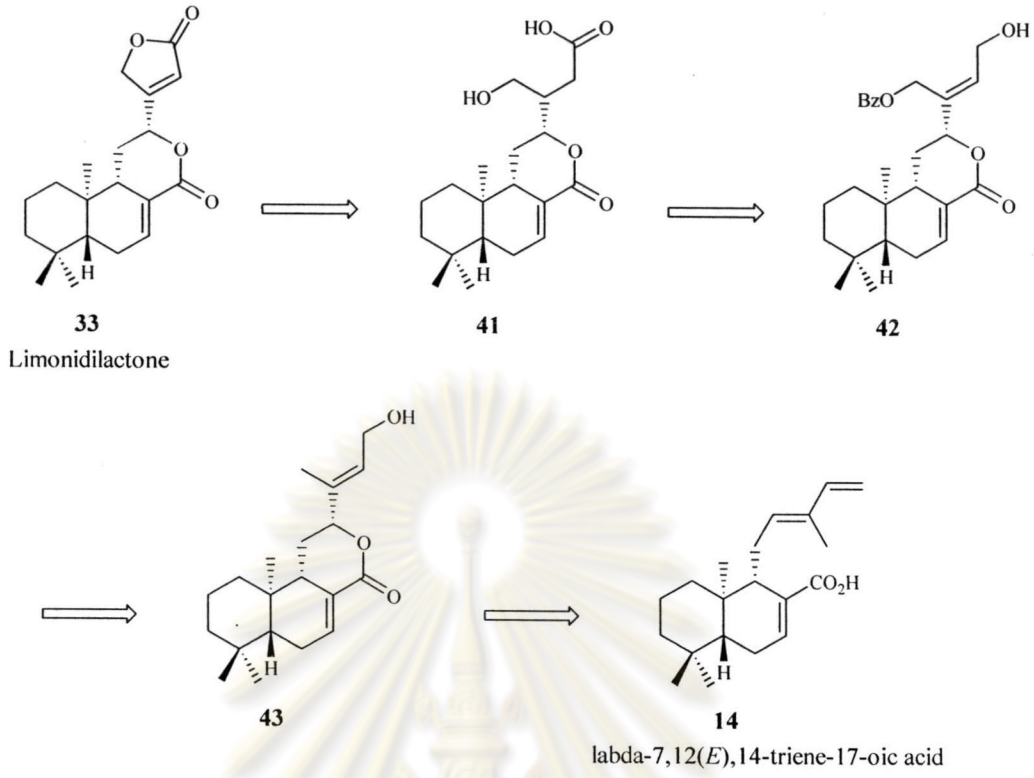

Scheme 3.6 Retrosynthetic plan for the synthesis of (+)-limonidilactone

Thus, allylic alcohol **52** was first synthesized by treating diene **14** with *m*-CPBA in the presence of $NaHCO_3$ as base (Scheme 3.7). However, this reaction gave the tertiary allylic alcohol **51** as a major product (63% yield) and the desired allylic alcohol **52** as a minor product (28% yield). It was subsequently thought to transform **51** into the desired allylic alcohol **52** by treatment with Lewis acid such as boron trifluoride (BF_3). Incidentally, when allylic alcohol **51** was treated with BF_3.2AcOH in dichloromethane, acetate **60** was found to be a product, the further intermediate, in 69% yield. Furthermore, an exposure of alcohol **52** with acetic anhydride (Ac_2O) in the presence of pyridine led to the same product in an excellent yield (100%). Consequently, the desired acetate **50** was obtained in 97% when combined the yields from allylic alcohols **51** and **52**.

It is known that SeO_2 is an effective oxidizing agent for the oxidation at allylic position [34]. So, the oxidation of the methyl group at C(16) position of acetate **60** with SeO_2 in the presence of TBHP in dichloromethane [35] was examined. Unfortunately, the reaction did not proceed as proposed ; only allylic alcohol **52** was obtained due to the removal of acetyl group when the reaction was carried out in EtOH [36].

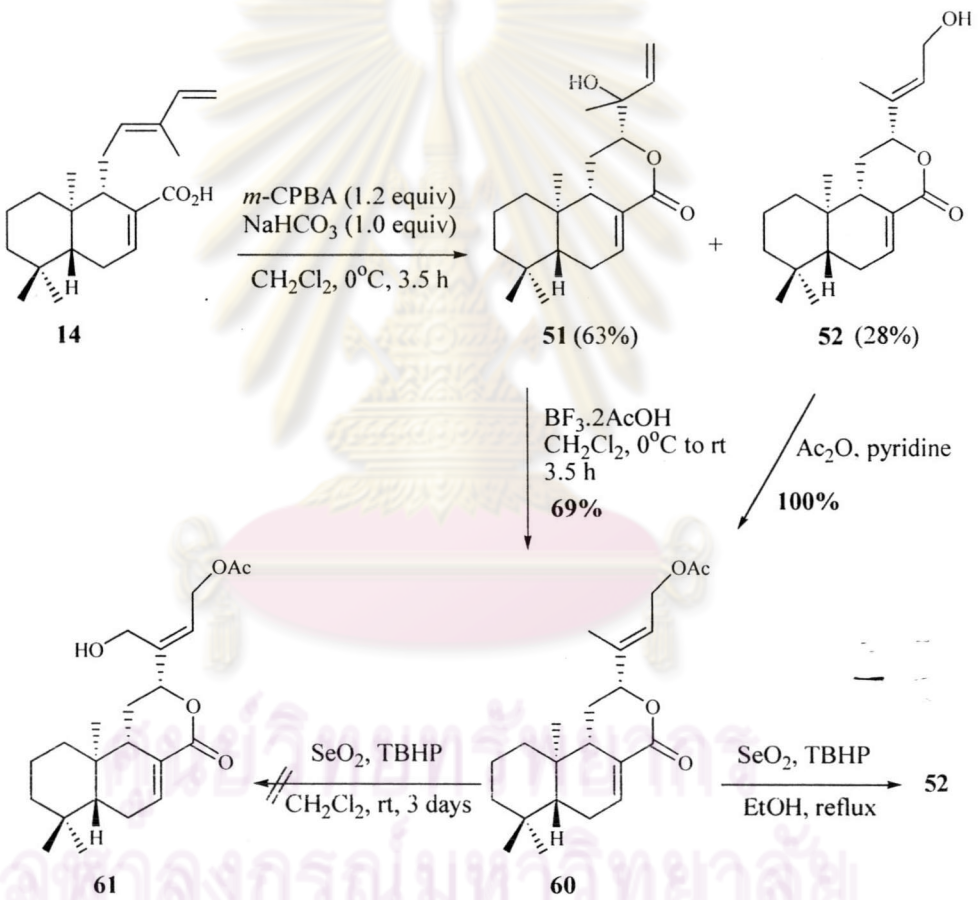

Scheme 3.7

Then, we decided to change the protecting group of C(15)-OH group. The silyl ether such as TBS was chosen since TBS ether could be stable for SeO_2 oxidation condition. A TBS group was thus installed on the C(15)-OH group of allylic alcohol **52** in 92% yield by treatment with TBSCl and imidazole [37]. However, the exposure of the TBS-protected derivative **62** to SeO_2 oxidation in EtOH at 50 °C gave only a disappointing result. The lost of TBS group also underwent under this condition leading to allylic alcohol **52** and the desired product **63** was not detected as shown in Scheme 3.8.

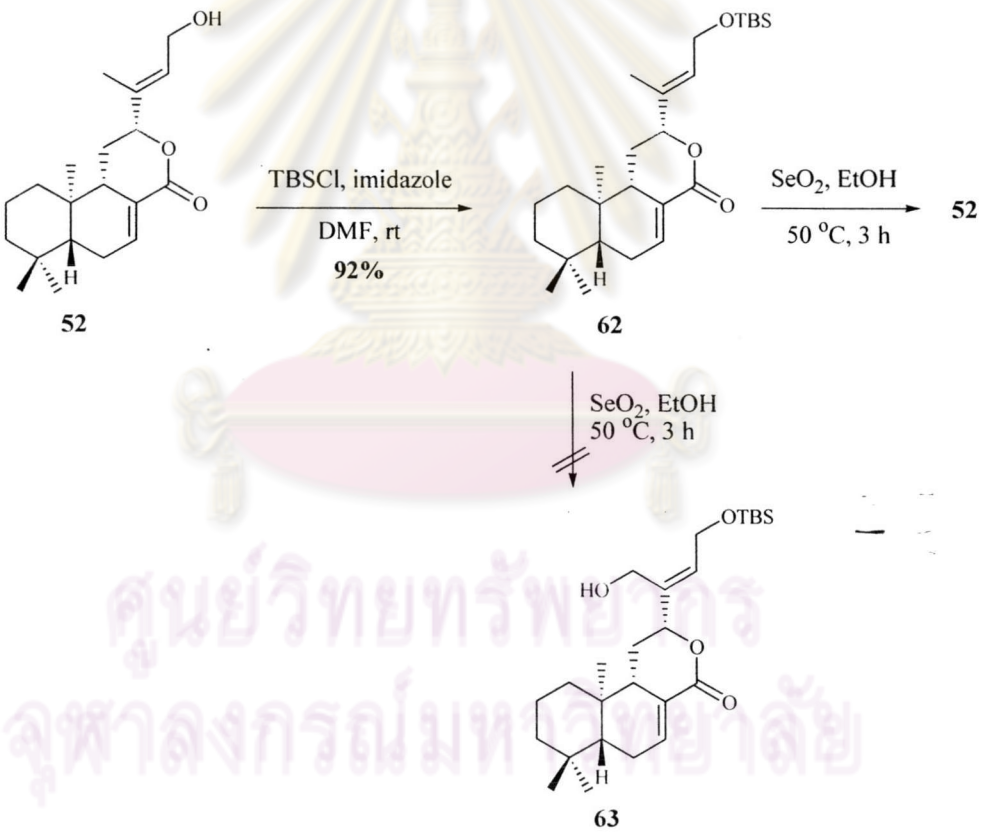

Scheme 3.8

In order to avoid the problem resulted from the cleavage of protecting group at C(15)-OH during SeO_2 oxidation, alternative lactonization between alcohol and ester functions was considered. In addition, it was anticipated that the ester group might be more versatile in terms of stability for SeO_2 oxidation in a harsher condition than the originally proposed acetoxy group. This prompted us to synthesize the methyl ester **65**, a precursor for lactonization. Fortunately, the cyanide-catalyzed MnO_2 oxidation of an α,β-unsaturated aldehyde to ester directly was well documented [38]. In the presence of HCN and CN^- a conjugated aldehyde was converted to the cyanohydrin which was further oxidized with active MnO_2 to an acyl cyanide leading to a final in an alcoholic medium to give ester as shown in Scheme 3.9. More importantly, this reaction proceeds in high yield without *cis-trans* isomerization of the α,β-olefinic linkage.

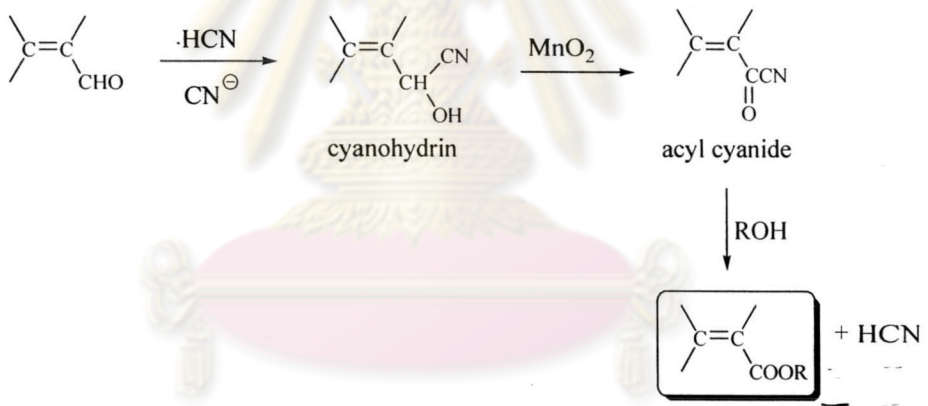

Scheme 3.9

The synthesis of methyl ester **65** was initiated by MnO_2 oxidation of allylic alcohol **52** to a conjugated aldehyde **64**. Without purification, the resulting aldehyde was then oxidized with MnO_2 in the presence of NaCN and AcOH to give the desired methyl ester **65** in 50% yield in 2 steps as shown in Scheme 3.10. It was thought that lactonization should be undertaken successively by following the introduction of a

hydroxyl group at C(16) position via SeO_2 oxidation. The construction of lactone ring system was then attempted by treatment of methyl ester **65** with SeO_2 in acetic anhydride. However, the oxidation could not be achieved even in a prolonged period of reaction time, which only the starting material was recovered.

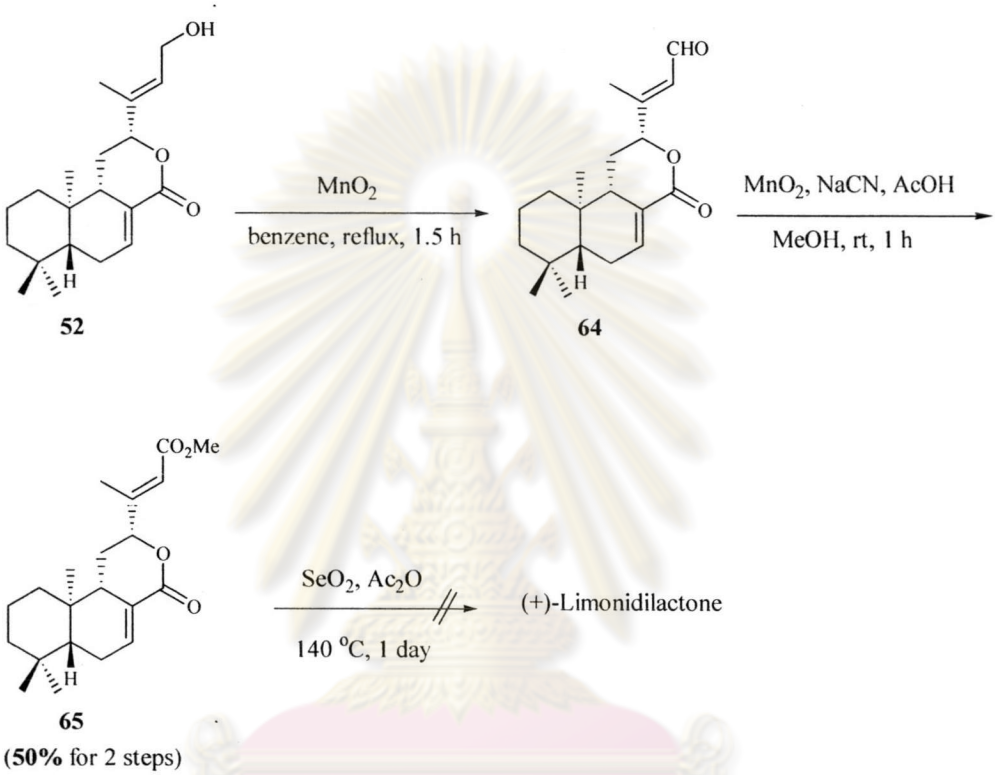

Scheme 3.10

Next, we turned our attention back to the oxidation of allylic acetoxy compound **60** with SeO_2 again. It is commonly known that, in the presence of anhydride as solvent, SeO_2 will undergo oxidation to give the protected allylic alcohol [39]. Therefore, the oxidation of the acetate **60** with SeO_2 in acetic anhydride was carried out and it was found that the reaction proceeded to furnish diacetate **66** as a mixture of *cis*- and *trans*-isomers, albeit in poor yield (28% yield) as shown in Scheme 3.11. However, the mixture of diacetates gave a complicated ^1H NMR spectrum. In

order to investigate the ratio of *cis*- and *trans*-isomers, the hydrolysis of a mixture of diacetates **66** was then carried out by treatment with 5% NaOH in EtOH, which resulted in a 66% yield of diols **67** with a clean ^{1}H NMR spectrum. Consequently, the ratio of *cis*- and *trans*-isomers was determined to be 0.12 to 1.0 by integration of the signal in the ^{1}H NMR spectrum of diols **67**.

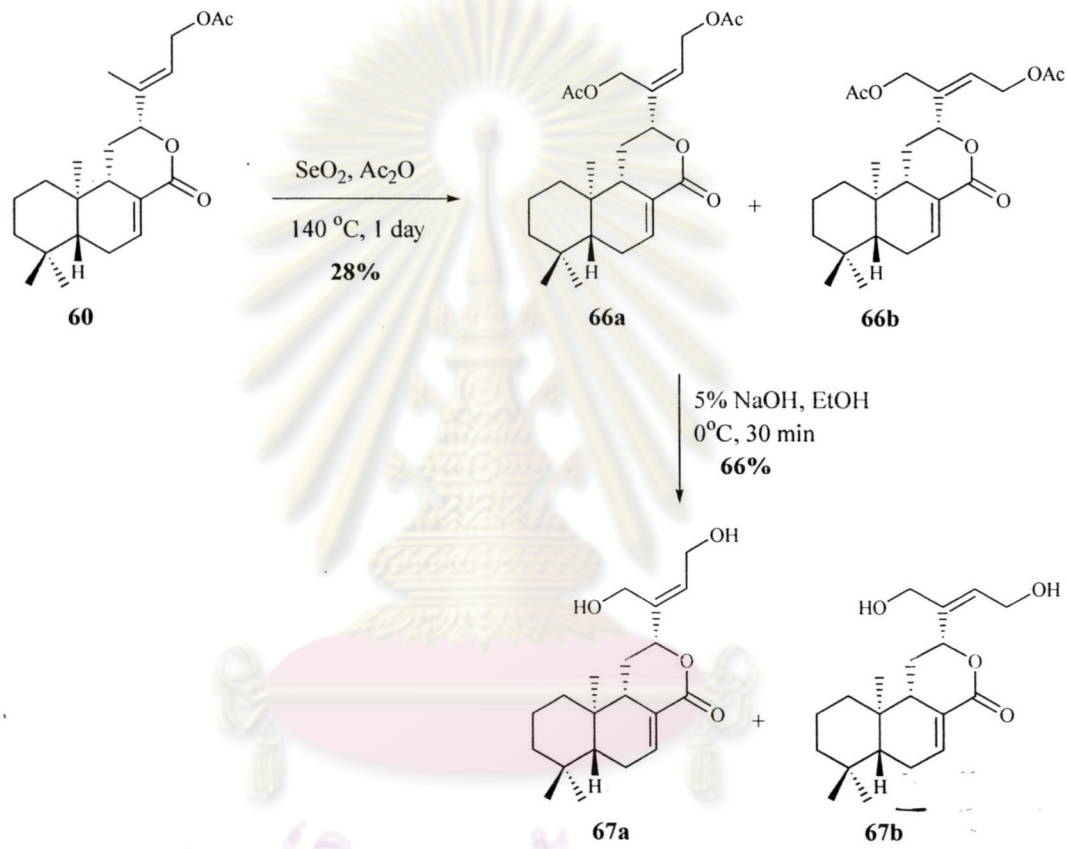

Scheme 3.11

We were able to determined the ratio of compound **66a** and **66b** in the mixture from the NOE experiment. From the experimental result, we discovered that **66b** existed in a higher ratio than **66a**. The NOE experimental result of **66b** is shown in Figure 3.5.

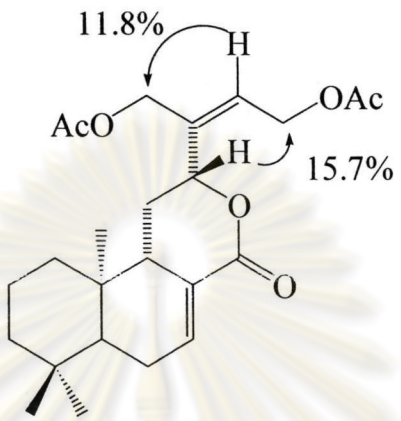

Figure 3.5 The NOE experiment of **66b**

Since diol **67** was considered to be employed as a precursor for the further step would be trouble. This due to the two hydroxyl groups of diol **67** which existed in the primary position and it would be difficult to find the condition that would provide a selective protection of either one of them. Therefore, we decided to change the solvent from SeO_2 oxidation of acetate **60** to producing the benzoyl acetate protected diol **68** as shown in Scheme 3.12. Disappointingly, the reaction gave very a low yield (17%) of the desired product **68** with a 0.17:1.0 mixture of *cis*- and *trans*-isomers. The ratio of the isomers was determined by integration of the ^1H NMR spectrum of a mixture of alcohols **69a** and **69b** which was obtained from the partial hydrolysis of a mixture of **68a** and **68b** to remove acetyl group by treating with 5% Na_2CO_3 in EtOH at room temperature.

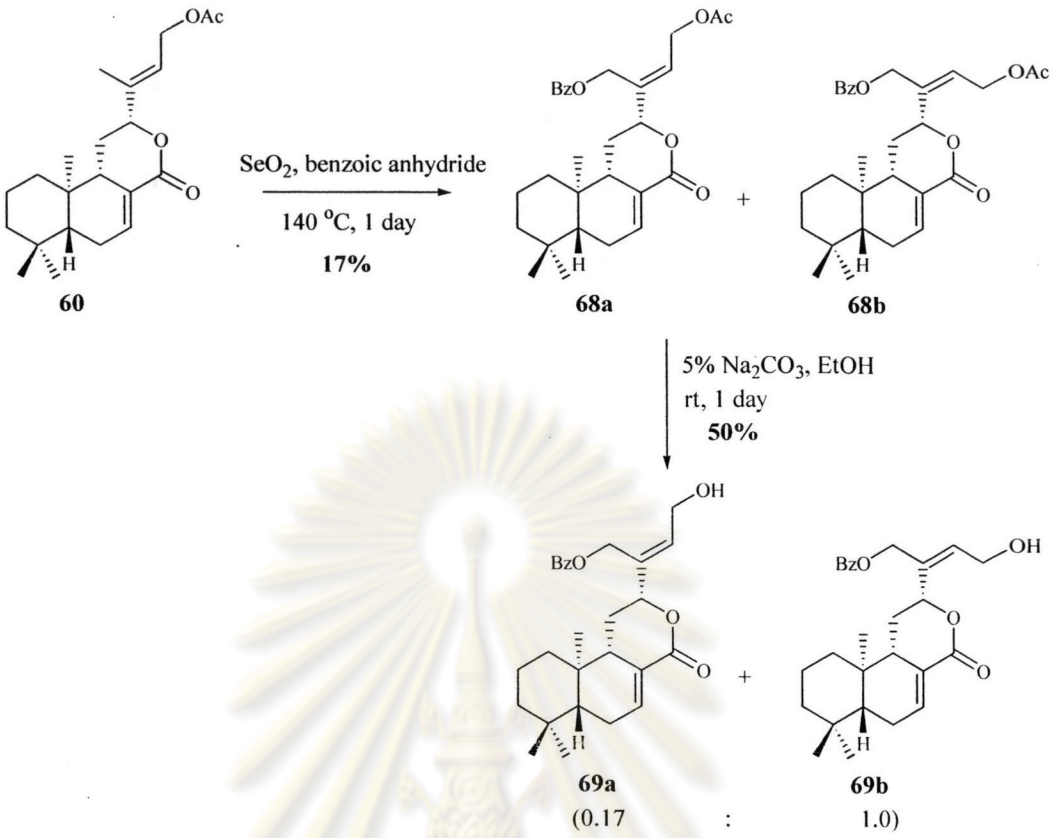

Scheme 3.12

From the above results, we thus decided to abandon this route because of the inability to improve the yield of the desired product. More importantly, only *cis*-isomer was required for the further lactonization, but it was obtained only a minor quantity from the oxidation of acetate **60** with SeO_2 in an anhydride.

However, a glimpse of the numerous failures encountered in attempting to introduce a hydroxyl group at allylic position onto our labdane diterpenes (**60**, **62**, and **65**) by using SeO_2 oxidation led us to consider its mechanism. It is known that the SeO_2 oxidation of olefin proceeds via 2,3-sigmatropic rearrangement of allylselenic acid generated from the reaction between SeO_2 and olefin as illustrated in Scheme 3.13 and gives allylic alcohol existing in *E*-configuration. In addition, this selective SeO_2 attack

to olefin was to be proven by Buchi and Wuest [40].

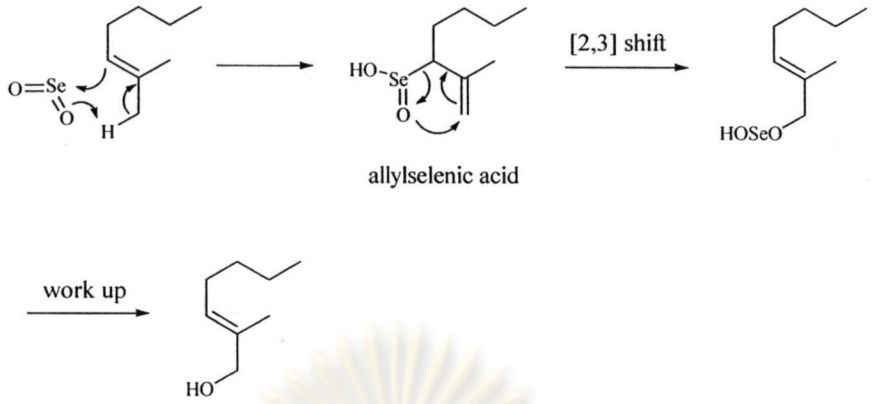

Scheme 3.13

Hence, it was supposed that SeO_2 oxidation of our labdane did not proceed as proposed because Me group existed in *Z*-configuration of double bond, which allylselenic acid could not be formed and 2,3-sigmatropic rearrangement could not occur as shown in Scheme 3.14.

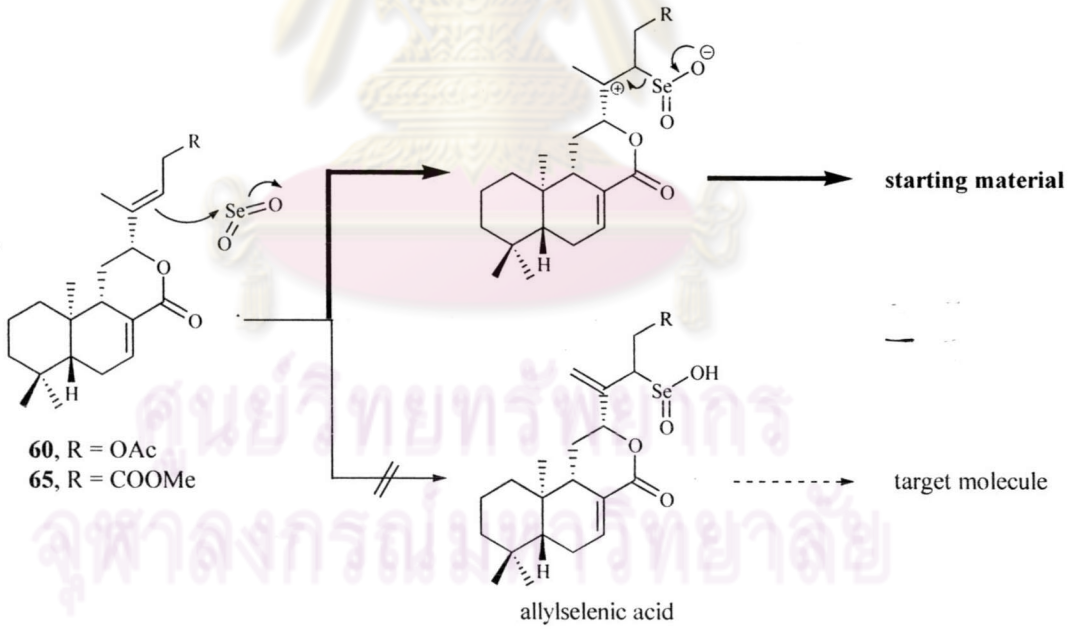

Scheme 3.14

Next, with an α,β-unsaturated methyl ester **65** in hands, we thus proposed to investigate the lactonization by utilizing the cyclization reaction of halo acid. Based on this concept, allylic bromination of methyl ester **65** must first be performed to produce bromo methyl ester **70** which would subsequently be converted to bromo acid **71**, a precursor for lactonization. Nevertheless, attempted bromination of methyl ester **65** with NBS in the presence of benzoyl peroxide as an initiator [41] was unsuccessful and led to many unidentified by-products which was indicated by TLC analysis, even when various solvent systems such as benzene, $CHCl_3$, and CCl_4 were used as shown in Scheme 3.15.

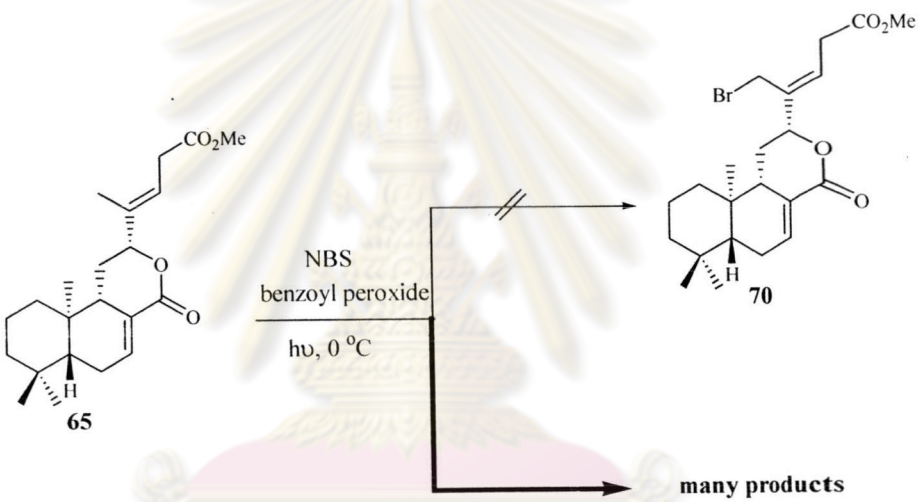

Scheme 3.15

Since all our attempts for introducing a hydroxy group at allylic C(16) position including allylic bromination failed , so it was decided to give up for futher investigation of this route.

As aforementioned, Marcos *et al* [23-24] reported the synthesis of limonidilactone (**34**) from a natural labdane diterpene, zarmoranic acid. Furthermore, we found that an enantiomer (**53**) of the first intermediate (**35**) in the synthetic pathway could be obtained in nearly quantitative yield upon exposure of labdane diterpene **14** to TsOH in

refluxing hexane as illustrated in Figure 3.6 [23-24]. Therefore, it was considered that the synthesis of (+)-limonidilactone from diterpene **14** should be accomplished according to this approach.

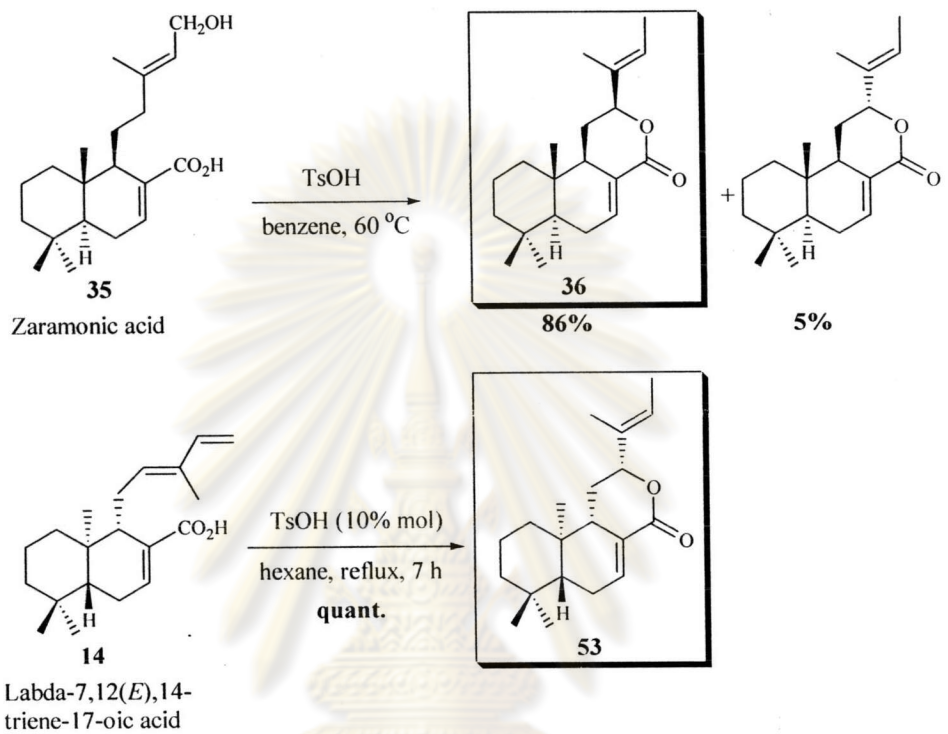

Figure 3.6

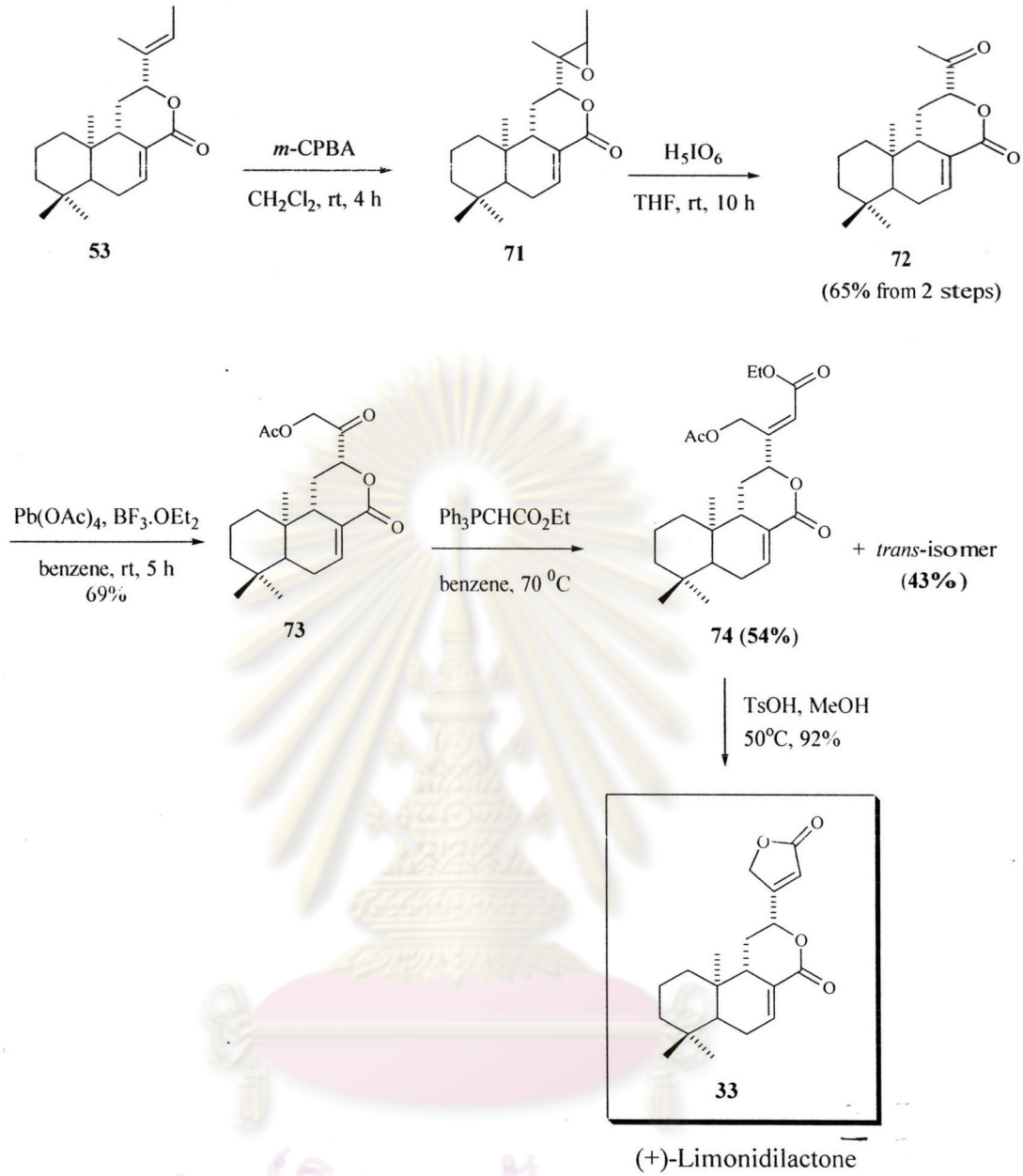

Scheme 3.16

To be accessible to (+)-limonidilactone, the epoxidation of olefin **53** with m-CPBA in dichloromethane was thus carried out which afforded a diastereomeric mixture of epoxide **71**. Without purification, the resulting epoxide was oxidized with H_5IO_6 to furnish methyl ketone **72** in 65% yield in 2 steps. Subsequent oxidation of

ketone **72** with $Pb(OAc)_4$ in the presence of $BF_3.OEt_2$ led to acetoxy ketone **73** as a single isomer in a moderate yield (69%). Then, the introduction of C(14) and C(15) to ketone **73** was performed through the Wittig reaction by treatment with Ph_3PCHCO_2Et and the desired *E*-isomer **74** was obtained in 54% yield accompanied by *Z*-isomer in 43% yield. Finally, the synthesis of (+)-limonidilactone **33** could be achieved in 92% yield by acid hydrolysis of compound **74** with TsOH in MeOH as shown in Scheme 3.16.

Based on spectroscopic and X-ray crystallography experiments, the absolutes configuration of (+)-limonilactone (**33**) was established as C9(*S*), C10(*R*) and C12(*R*) showed in Figure 3.7. After comparison of the ^{1}H NMR spectroscopy of compound 33 with limonidilactone described by Aphaijitt and Marcaos, it suggested that the structure of compound **33** should be same the reported by Marcos et al. The ^{1}H NMR spectrum of compound **33** and (+)-limonidilactone (Marcos') showed a single signal of H-16 at 4.94 and 4.95 ppm, respectively while the H-16 signal of (-)-limonidilactone (Aphaijitt's) was split into 2 peaks at 4.96 and 4.97 ppm as shown in Table 3.3.

In addition, it was subsequently confirmed that both were the same compound by measuring their optical rotation which showed as +14.2 (Marcas') and +14.0 (compound **33**). Consequently, compound **33** was (+)-limonidilactone whose absolute configuration was established as C9(*S*), C10(*R*), C12(*R*), not C9(*R*), C10(*S*), C12(*S*) as Marcos reported. As well as the absolute configuration of the nature (-)-limonidilactone isolated by Aphaijitt could be clearly established as C9(*R*), C10(*S*), C12(*S*) as shown in Figure 3.7.

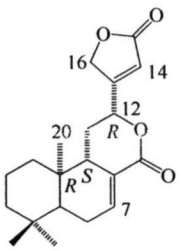

(+)-Limonidilactone

The optical rotation as plus (+)

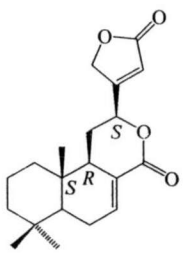

(-)-Limonidilactone

The optical rotation as minus (-)

reported by Aphaijitt *et al*

Figure 3.7

Table 3.3 Comparison of the ^{1}H NMR data and optical rotation of limonidilactone

		Limonidilactone		
		Aphaijitt	Marcos	**33**
ppm (δ)	H-7	7.40	7.41	7.40
	H-12	5.25	5.21	5.21
	H-14	6.10	6.08	6.07
	H-16	4.96, 4.97	4.95	4.94
	Me-20	0.78	0.78	0.76
$[\alpha]_D$		-23.8	+14.2	+14.0

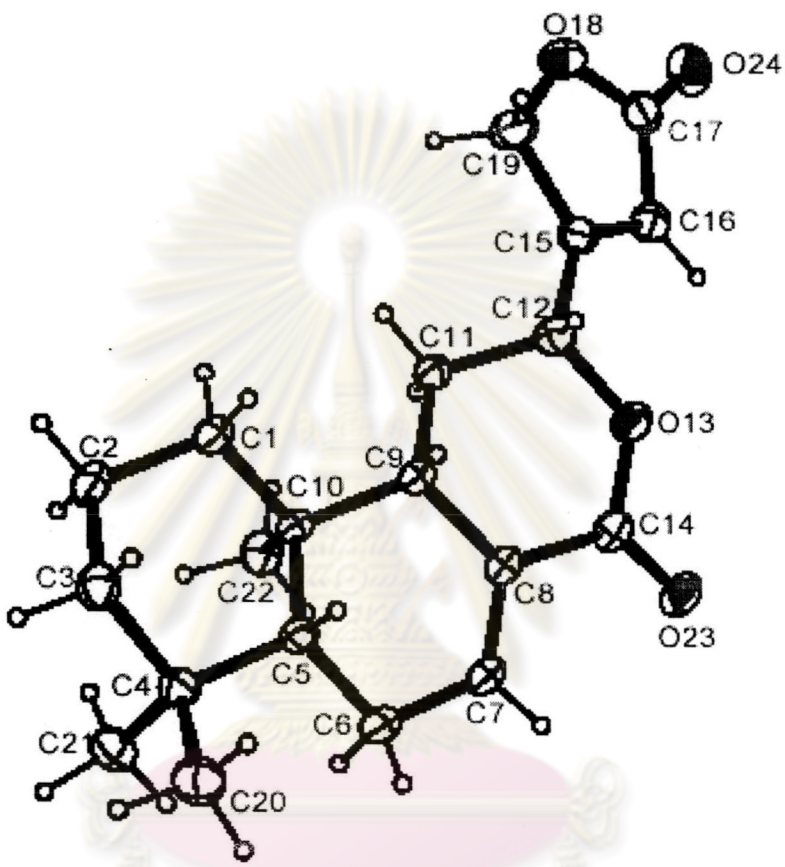

Figure 3.8 The structure of (+)-limonidilactone (**33**) from X-ray analysis.

3.4 Biological Activities of Modified Labdanes

We would like to discuss the cytotoxicity and inhibitory effect of Na^+, P^+-ATpase of natural labdanes and their derivatives.

3.4.1 Cytotoxic activity of modified labdanes

The bioassay of cytotoxicity against human cell cultures in vitro was performed by the MTT[3-(4,5-dimethylthiazol-2-yl)-2,5-diphenyltetrazolium bromide] colorimetric method [42]. Doxorubicin hydrochloride was used as a positive control substance.

Fourteens compounds **11-14** and **47-56** were tested for their cytotoxicity against human tumor cell lines (Table 3.4) and found that compounds **12, 13, 48, 53** and **54** showed non-specific moderate cytotoxicity against human breast ductol carcinoma (BT474), human undifferentiated lung carcinoma (CHAGO), human liver hepatoblastoma (HEP-G2), gastric carcinoma (KATO3), and colon adenocarcinoma (SW620). Compounds **11, 14, 47, 49, 50, 51, 55** and **56** were inactive against all cell lines (> 10 μg/ml) [43]. Compound **52** showed weak activity against gastric carcinoma (7.6 μg/ml) and was inactive against liver hepatoblastoma (> 10 μg/ml) while compound **54** showed strong activity against gastric carcinoma (0.6 μg/ml) and breast ductol carcinoma (2.5 μg/ml). It is very interesting to see that **54** is more selective than compounds **12, 13, 48, 52** and **53.** The activity of compound **12** is likely due to the α,β-unsaturated aldehyde which could undergo Michael addition with nucleophilic group in proteins and DNA. Compounds **21, 22** and **26** (chapter 1) represent some examples with the *α,β*-unsaturated carbonyl moiety which showed cytotoxic activity against human cancer cell lines. The other active compounds (such as compounds **13, 48, 52, 54** and **56**) possess primary allylic alcohol moiety which presumably is the essential for its cytotoxic activity. This information is agreed to those of cytotoxic

labdane diterpenoids reported by Demetzos *et al.* [16-17]. The possible explanation is that the allylic alcohol could be oxidized *in vivo* to α,β-unsaturated aldehyde which then acts as a Michael acceptor as compound **12**. For compound **53**, there is no clear explanation for its cytotoxic activity.

Table 3.4. Cytotoxicity data for compounds **11-14** and **47-56**[a]

	Cell lines[b]				
Compounds	BT474	CHAGO	HEP-G2	KATO3	SW620
11	>10	>10	>10	>10	>10
12	5.0	4.8	5.2	4.2	5.5
13	5.4	5.8	6.3	5.8	5.7
14	>10	>10	>10	>10	>10
47	>10	>10	>10	>10	>10
48	4.7	5.7	6.5	5.3	5.6
49	>10	>10	>10	>10	>10
50	>10	>10	>10	>10	>10
51	>10	>10	>10	>10	>10
52	5.9	6.0	>10	7.6	6.0
53	4.9	6.4	6.0	4.6	5.0
54	2.5	6.1	5.3	0.6	6.1
55	>10	>10	>10	>10	>10
56	>10	>10	>10	>10	>10
Doxorubicin hydrochloride	0.08	2.3	0.9	1.7	1.1

[a] Results are expressed as IC_{50} values (μg/ml)

[b] BT-474, human breast ductol carcinoma ATCC No. HTB 20:

CHAGO, human undifferentiated lung carcinoma;

HEP-G2, human liver hepatoblastoma ATCC No. HB 8065;

KATO-3, human gastric carcinoma ATCC No. HTB 103;

SW620, human colon adenocarcinoma ATCC No. CCL 227

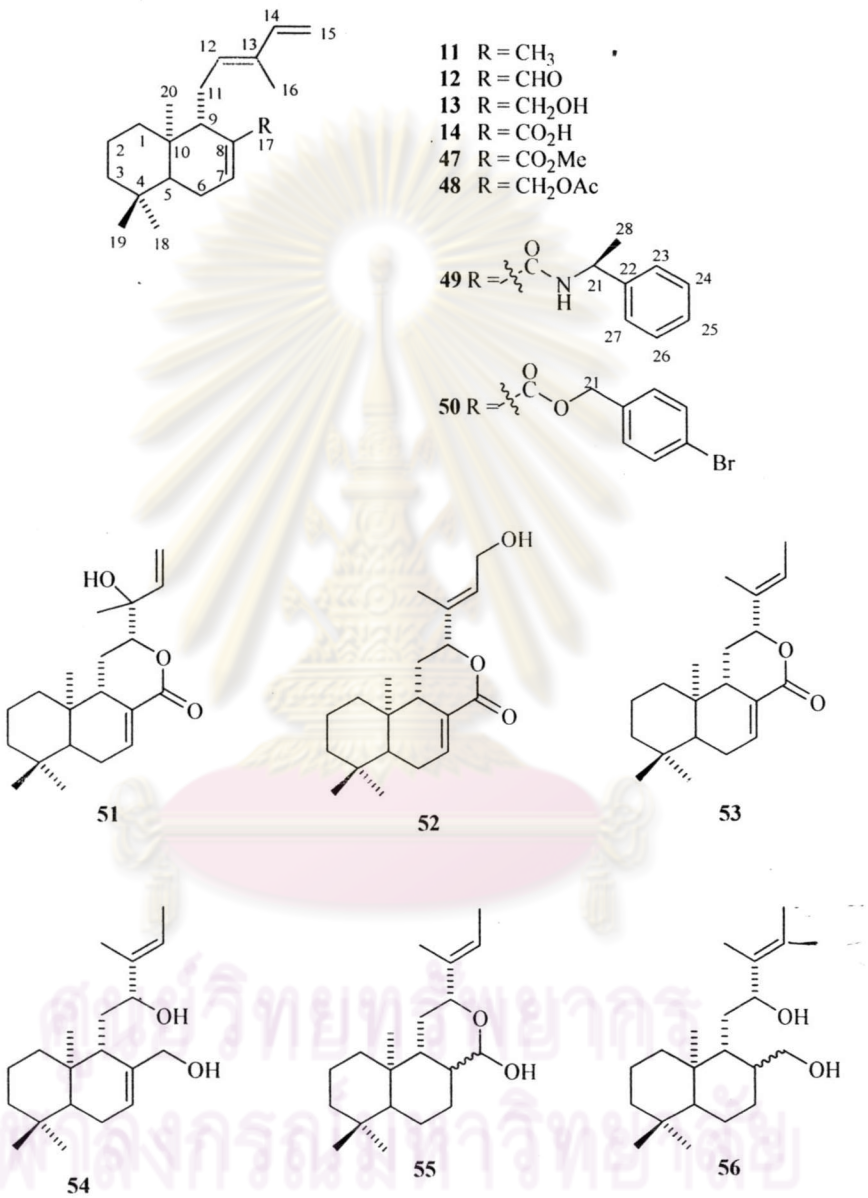

Figure 3.9 The structure of labdane compounds for test the biological activity

3.4.2 The inhibitory effect of Modified Labdanes on Na^+-K^+-ATPase.

Selected natural labdanes which were isolated from *C. oblongifolius* and their derivatives were tested biological activity on Na^+, K^+-ATPase assay to look for anti-Alzheimer and diuretic drugs. Compounds **13**, **14**, **47**, **48**, **49**, **50**, **51**, **52**, **53**, **55** and **56** were dissolved in DMSO and added to the reaction tube each 2 μL. The structure showed in Figure 3.9.

From 3 rats, weighted about 317 g/rat, were separated brain 2.14 g and kidney 6.71 g. From rat brain, it was isolated crude enzyme Na^+, K^+-ATpase 16.72 mg protein (specific activity 2.6μmol Pi/mg protein/min). From rat kidney, it was isolated as crude Na^+, K^+-ATPase 66.80 mg protein (specific activity 1.47 μmol Pi/mg protein/min). The optimum concentration of the crude enzyme from rat brain and rat kidney was 5 μg/μL. The optimum incubation time of crude enzyme from rat brain was 15-30 min. and from rat kidney was 15 min.

Rat brain and rat kidney were inhibited completely by 10^{-2} M of ouabain. A 50 % inhibition with the rat brain and rat kidney enzyme were reached at an ouabain concentration 2.0×10^{-7} M and 9.0×10^{-5} M, IC_{50} value respectively.

From the above results, we selected crude enzyme Na^+, K^+-ATPase from rat brain for testing samples because Na^+, K^+-ATPase from rat brain showed higher specific activity than that from rat kidney under condition as following : [enzyme] 5 μg/100 μL, incubation time 30 min, 0.01 M ouabain with 140 mM NaCl and 14 mM KCl.

The result of crude enzyme Na^+, K^+-ATPase from rat brain showed in Table 3.5.

Table 3.5. Inhibition of Modified labdanes on crude enzyme Na^+, K^+-ATPase from rat brain

Compounds	IC_{50} values
13	9.0×10^{-5}
14	5.0×10^{-5}
47	5.8×10^{-4}
48	3.0×10^{-4}
49	1.0×10^{-4}
50	2.5×10^{-4}
51	2.5×10^{-4}
52	2.2×10^{-4}
53	2.5×10^{-4}
55	$> 1.0 \times 10^{-3}$
56	$> 1.0 \times 10^{-3}$

Compounds **13** and **14** showed strong inhibitory activity, whereas compounds **47-53** showed moderate inhibitory activity and compounds **55** and **56** showed no inhibitory activity on crude enzyme Na^+, K^+-ATPase.